

Edge channel mixing induced by potential steps in an integer quantum Hall system

D. Venturelli

*Institut NEEL, CNRS and Université Joseph Fourier, Boite Postale 166, 38042 Grenoble, France
NEST, Istituto Nanoscienze-CNR & Scuola Normale Superiore, Piazza dei Cavalieri 7, I-56126 Pisa, Italy
International School for Advanced Studies (SISSA), Via Beirut 2-4, I-34014 Trieste, Italy*

V. Giovannetti, F. Taddei and R. Fazio

NEST, Istituto Nanoscienze-CNR & Scuola Normale Superiore, Piazza dei Cavalieri 7, I-56126 Pisa, Italy

D. Feinberg

Institut NEEL, CNRS and Université Joseph Fourier, Boite Postale 166, 38042 Grenoble, France

G. Usaj and C. A. Balseiro

*Centro Atómico Bariloche and Instituto Balseiro,
Comisión Nacional de Energía Atómica, 8400 S. C. de Bariloche, Argentina
(Dated: October 9, 2022)*

We investigate the coherent mixing of co-propagating edge channels in a quantum Hall bar produced by step potentials. In the case of two edge channels it is found that, although a single step induces only a few percent mixing, a series of steps could yield 50% mixing. In addition, a strong mixing is found when the potential height of a single step allows a different number of edge channels on the two sides of the step. Charge density probability has been also calculated even for the case where the step is smoothened.

PACS numbers:

I. INTRODUCTION

When a two dimensional electron gas (2DEG) is subject to a large magnetic field, the integer quantum Hall (IQH) regime is accessed. Here charge transport is allowed by the formation of edge-state channels, each accounting for a single quantum of conductance. As pointed out for the first time in Refs. 1, this system became the prototype of a single-channel conductor with spectacular properties such as chirality and adiabatic transport, whose study fueled an enormous amount of work in the field of nanoscience². Recently, phase-coherence was studied and found to be preserved over rather long distances, of the order of more than 10 micrometers³. For this reason 2DEGs in the IQH regime appear to be specially suited for electronic interferometry, a very stimulating phenomenon both for basic science and for its various possible applications. A recent breakthrough in this field has been the experimental realization of electronic Mach-Zehnder⁴⁻⁸ and Hanbury-Brown and Twiss⁹ interferometers. In these experiments electrons in the edge states loop around an annular structure mimicking the optical paths of their photonic counterparts.

Recently, a new theoretical scheme was proposed¹⁰ which would allow for a concatenation of several Mach-Zehnder interferometers (MZIs) in series. This new opportunity of scalability, which is not topologically possible in any of the setups experimentally developed so far, exploits the interference between adjacent edge channels with the same chirality, coupled by means of some localized potential. While the possibility of locally breaking the adiabatic transport in IQH systems has been recog-

nized long time ago¹¹, there is now a call for a more focused study on how much adjacent co-propagating edge channels might be influenced by an engineered non-adiabatic potential.

In this paper we investigate the possibility of inducing coherent mixing between two co-propagating edge channels in a Hall bar due to abrupt (non-adiabatic) potential steps along the direction of propagation. The implementation of such local, short-scale potential variations is, in principle, within the experimental reach of cutting-edge technology, for example, through: i) precise impurity implantation by means of focused ion beam¹⁵, AFM induced oxidation¹⁶, cleaved-edge overgrown technique¹⁷, and tunable scanning gate microscopy¹⁸.

For the sake of clarity here we focus on idealized configurations. We first consider the case of a single potential step where two edge channels are open on its left and right hand side, finding that the channel mixing probability is pretty small even for heights of the potential step of the order of the Landau level (LL) separation $\hbar\omega_c$. Moreover, in the presence of a single edge channel on both sides of the step, we find that no reflection is allowed as long as the width of the bar is larger than a few magnetic lengths. By placing in series a number of such potential steps, though, channel mixing of the order of 50% could realistically be achieved. The situation changes when a single edge channel is open on the left hand side, while two channels are open on the right hand side of a potential step. Here channel mixing can be as high as 30% for a sharp step. Finally we calculate the stationary charge density in the Hall bar even in the case where the potential step is smoothed, finding indi-

cations, in all situations examined, that channel mixing persists (within the same order of magnitude) as long as the potential changes over a distance not exceeding few magnetic lengths.

The paper is organized as follows. In Sec. II we specify the system under study and we describe the numerical technique used for our calculations. In Sec. III we discuss the results obtained when the abrupt step potential connects two regions characterized by the same edge filling factor (III A), and in the case of a series of such steps (III B). In Sec. III C we consider the case with one open channel on the left and two open channels on the right. Finally, Sec. IV finally focuses on the charge density probability produced by the presence of the step potential, even in the case when it is smooth.

II. MODEL AND NUMERICAL TECHNIQUE

The system under investigation consists of a quantum Hall bar subjected to a sharp step-like potential $U(y)$ along the longitudinal y direction (see Fig. 1), whose role is to induce scattering among otherwise independent edge-state channels. In the following we will neglect the spin degree of freedom of the electrons, settling the notation on “orbital” edge channels. The latter are determined through the eigenfunctions of the time-independent Schrödinger equation $H\Psi(x, y) = E\Psi(x, y)$ with the single-electron Hamiltonian (in Landau gauge) given by

$$H = \frac{\hbar^2}{2m} \left[-\frac{\partial^2}{\partial x^2} + \left(-i\frac{\partial}{\partial y} + \frac{|e|B}{c\hbar}x \right)^2 \right] + U(y), \quad (1)$$

where e and m are, respectively, the electron charge and the effective electron mass, B is the perpendicular magnetic field. A hard wall confinement potential that defines the edges of the sample is assumed. In Eq. (1) $U(y)$ is the step potential function which is taken to be zero for $y < 0$ (region I) and constant for positive y (region II), i.e. $U(y) = -\Delta E \Theta(y)$, where $\Theta(y)$ is the Heaviside function. Under these conditions the Hall bar effectively splits into two regions and the resulting scattering problem can be solved through a *mode matching* method¹⁹ as detailed in the following.

First we notice that in both regions the eigenfunctions of the Hamiltonian can be expressed as scattering states in the y -direction (i.e. $\Psi(x, y) = \psi(x)e^{iky}$) which formally differ just for their “effective energy”: $E_{eff}^I = E$ for region I and $E_{eff}^{II} = E + \Delta E$ for region II. Here E is the energy of the propagating incoming electrons (defined so that the first LL corresponds to $E = \hbar\omega_c/2$, where $\omega_c = |e|B/cm$ is the cyclotron frequency), while $E + \Delta E$ is the energy of the outgoing electrons. Therefore the time-independent Schrödinger equation reduces to

$$\left[-\frac{\partial^2}{\partial x^2} + (k + \beta x)^2 - \epsilon^i \right] \psi(x) = 0, \quad (2)$$

where $i = I, II$ specifies the region, $\beta = l_B^{-2} = |e|B/c\hbar$ is the inverse magnetic length squared, $\epsilon^i = 2mE_{eff}^i/\hbar^2 = 2\beta (E_{eff}^i/\hbar\omega_c)$ is the rescaled effective energy. The solutions for the transverse eigenfunction ψ are completely specified by the magnetic field and by imposing hard wall boundary conditions: $\psi(x = -L/2) = \psi(x = L/2) = 0$. The resulting expression is a transcendental equation that can be expressed in analytic form in terms of parabolic cylinder functions²⁰. We opt nevertheless for a numerical solution following a similar technical strategy as the one detailed in the appendix of Refs. 19.

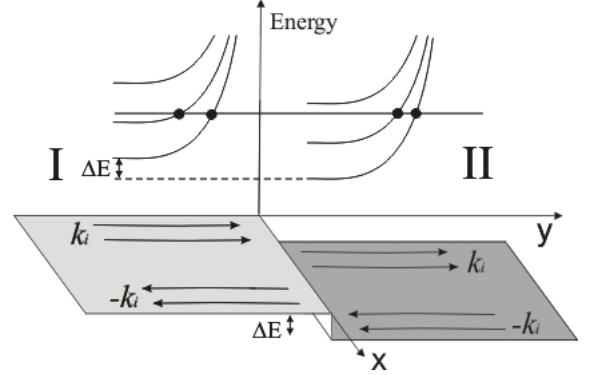


Figure 1: Schematics of the set-up. A hard wall potential confines the 2DEG in the transverse direction defined by the coordinates $x \in [-L/2, L/2]$. Along the longitudinal direction y a step potential $U(y)$ is introduced to induce coherent mixing among the propagating modes. Its effect is accounted as a global energy shift between the solutions of the Schrödinger equation in the two regions, as pictured on the dispersion band curves of the edges drawn on the background of the figure (the horizontal line that intersects the bands indicates the Fermi energy).

In both regions, for a given ϵ^i one can find a set of complex values for the wave-vector k satisfying Eq. (2). Those with zero imaginary part are associated to propagating longitudinal wave-functions which correspond to the $2P_i$ edge-state channels. P_i represents the LL filling factor of region i , defined by the integer part of the quantity $E_{eff}^i/\hbar\omega_c + \frac{1}{2}$ (notice that since E_{eff}^i differs in the two regions, P_I and P_{II} need not to coincide). More precisely, we can identify P_i real positive solutions $\{k_n^i; n = 1, \dots, P_i\}$ that describe propagating right-going channels $\{\psi_n^{Ri}(x); n = 1, \dots, P_i\}$, and P_i real negative solutions $\{-k_n^i; n = 1, \dots, P_i\}$ that describe propagating left-going channels $\{\psi_n^{Li}(x); n = 1, \dots, P_i\}$. Such modes are responsible for the electronic transport in the sample. We normalize them in such a way that their current flux is unity. This means that we impose:

$$\int_{-L/2}^{L/2} dx [\psi_n^{Ri}(x) (k_n^i - eA_x) \psi_n^{Ri}(x)^*] = 1 \quad (3)$$

where $A_x = \beta x/e$ is the only non-zero component of the vector potential in the Landau gauge. The normalization

of $\psi_n^{Li}(x)$ follows by the symmetry of the problem that imposes $\psi_n^{Li}(x) = \psi_n^{Ri}(-x)$ for all n and i . The complex and purely imaginary solutions, instead, are associated with evanescent eigenfunctions $\bar{\psi}_n^i$ of the system. They do not contribute directly to the net electronic transport but are needed to guarantee the continuity of the wave-function and of the probability current when imposing the matching conditions to the solutions²¹,

$$\begin{aligned}\Psi^I(x, y=0) &= \Psi^{II}(x, y=0), \\ \partial_y \Psi^I(x, y=0) &= \partial_y \Psi^{II}(x, y=0).\end{aligned}\quad (4)$$

A generic solution of the Schrödinger equation can thus be written as follows

$$\begin{aligned}\Psi^i(x, y) &= \sum_{n=1}^{P_i} a_n^i \psi_n^{Ri}(x) e^{ik_n^i y} + \sum_{n=1}^{P_i} b_n^i \psi_n^{Li}(x) e^{-ik_n^i y} \\ &+ \sum_{n=1}^{M_i} c_n^i \bar{\psi}_n^i(x) e^{i\bar{k}_n^i y},\end{aligned}\quad (5)$$

where \bar{k}_n^i are the complex wave-vectors of the evanescent modes $\bar{\psi}_n^i$. We stress that in principle such expansion should take into account *all* the evanescent modes associated with the selected value of E_{eff}^i . However, since the latter are infinitely many, to make the problem treatable numerically we limit the value of M_i to only include all modes whose \bar{k}_n lies within a finite radius from the origin of the complex plane¹⁹. This way we always expand over all the exponentially damped oscillating modes (i.e. the \bar{k}_n with finite real *and* imaginary components) and a certain given number of purely-imaginary wave-vector evanescent modes, under the condition that the final results do not vary significantly if new evanescent modes are added in the expansion.

Consider first the case of small ΔE , i. e. where the potential step maintain the same filling factor in the two regions (i.e. $P_I = P_{II} = P$), and focus on the scattering process associated with right-going electrons coming from the left lead with given mode number $j \in \{1, 2, \dots, P\}$. Due to the normalization convention Eq. (3), the scattering amplitudes t_{nj} (r_{nj}) that couple such incoming mode with the transmitted (reflected) modes in the channel n , can then be directly identified with the coefficients a_n^{II} (b_n^I), that one obtains from Eq. (5) while imposing the matching conditions (4) at the boundary. The number of unknowns is given by $2(P + M)$, since, although not entering in the scattering matrix, the coefficients relative to evanescent waves (c_n^I and c_n^{II}) must be found. The $2(P + M)$ equations needed to determine them can be set by expanding the functions $\psi_n^{Ri}(x)$, $\psi_n^{Li}(x)$ and $\bar{\psi}_n^i(x)$ in the first $N/2 = (P + M)$ Fourier

modes $\varphi_n = \sqrt{\frac{1}{L}} \sin\left(\frac{n\pi x}{L}\right)$ as follows:

$$\psi_n^{Ri}(x) = \sum_{j=1}^{N/2} \alpha_{nj}^i \varphi_j(x) \quad \text{for } 1 \leq n \leq P, \quad (6)$$

$$\psi_n^{Li}(x) = \sum_{j=1}^{N/2} \beta_{nj}^i \varphi_j(x) \quad \text{for } 1 \leq n \leq P, \quad (7)$$

$$\bar{\psi}_n^i(x) = \sum_{j=1}^{N/2} \gamma_{nj}^i \varphi_j(x) \quad \text{for } 1 \leq n \leq M, \quad (8)$$

the coefficients α_{nj}^i corresponding to right-going modes, β_{nj}^i to left-going modes, and γ_{nj}^i to evanescent modes. At the end of the simulation we check that the number of Fourier Modes used in the expansion is sufficient to properly describe all propagating, oscillatory damped and evanescent modes that contribute appreciably to the scattering matrix. By multiplying by φ_l and integrating over x , the above expressions can be recasted in the following $N \times N$ matrix equation:

$$\begin{aligned}&\begin{pmatrix} \sum_n^P (a_n^I \bar{\alpha}_{nl}^I - a_n^{II} \bar{\alpha}_{nl}^{II}) \\ \sum_n^P (k_n^I a_n^I \bar{\alpha}_{nl}^I - k_n^{II} a_n^{II} \bar{\alpha}_{nl}^{II}) \end{pmatrix} = \\ &= \begin{pmatrix} \mathcal{B}^{II} & -\mathcal{B}^I & \mathcal{G}^{II} & -\mathcal{G}^I \\ \tilde{\mathcal{B}}^{II} & -\tilde{\mathcal{B}}^I & \tilde{\mathcal{G}}^{II} & -\tilde{\mathcal{G}}^I \end{pmatrix} \begin{pmatrix} \bar{b}_n^{II} \\ \bar{b}_n^I \\ \bar{c}_n^I \\ \bar{c}_n^{II} \end{pmatrix}\end{aligned}\quad (9)$$

where for $i = I, II$, $\bar{\alpha}_{nl}^i \equiv (\alpha_{n1}^i, \alpha_{n2}^i, \dots, \alpha_{nN}^i)^T$, $\bar{b}_n^i \equiv (b_{n1}^i, b_{n2}^i, \dots, b_{nP}^i)$, $\bar{c}_n^i \equiv (c_{n1}^i, c_{n2}^i, \dots, c_{nM}^i)$, and \mathcal{B}^i , \mathcal{G}^i denote the matrices containing the Fourier coefficients, namely $(\mathcal{B}^i)_{nl} \equiv \beta_{nl}^i$ and $(\mathcal{G}^i)_{nl} \equiv \gamma_{nl}^i$ respectively, while $\tilde{\mathcal{B}}^i$ and $\tilde{\mathcal{G}}^i$ denote the matrices of elements $(\tilde{\mathcal{B}}^i)_{nl} \equiv k_n^i \beta_{nl}^i$ and $(\tilde{\mathcal{G}}^i)_{nl} \equiv k_n^i \gamma_{nl}^i$. This linear problem can be solved numerically so that the resulting coefficients allow a full reconstruction of the wave-function in all regions through Eq. (5). In the next section we shall apply this procedure for $P = 1$ and $P = 2$. The same analysis holds when $P_I \neq P_{II}$ with the only important requirement that the linear system in Eq. (9) is determined, i.e. that $P_I + M_I \equiv P_{II} + M_{II}$. An example of such configuration is presented in Sec. III C where we assumed $P_I = 1$ and $P_{II} = 2$.

To conclude the section we mention that the conductance G of the system is determined, according to the Landauer-Büttiker scattering theory¹, by the expression

$$G = \frac{2e^2}{h} \sum_{n=1}^{P_{II}} \sum_{j=1}^{P_I} |t_{nj}|^2, \quad (10)$$

valid in limit of small voltages and zero temperature.

III. RESULTS

In this section we shall discuss the results obtained for the scattering amplitudes in the case of a Hall bar with either one or two open edge channels.

A. Two regions with equal filling factor

Let us now consider the case of two edge channels ($P_I = P_{II} = 2$) on each side of the step potential, aiming at evaluating the channel mixing probabilities $|t_{12}|^2$ and $|t_{21}|^2$ representing the probability for transmission from inner (2) to outer (1) edge and vice-versa, respectively (see Fig. 1). By setting $L = 6.7l_B$, where $l_B = \beta^{-\frac{1}{2}}$ is the magnetic length, we make sure that the reflection probabilities are negligible. More precisely, fixing the energy of the incoming electrons at $1.7\hbar\omega_c$ above the first LL, we found that the only non-vanishing, though very small, reflection coefficient is $|r_{22}|^2 \sim 10^{-3}$. In Fig. 2 the channel mixing probability $|t_{12}|^2$ is plotted as a function of the potential barrier height ΔE in units of $\hbar\omega_c$. $|t_{12}|^2$ increase monotonically with increasing ΔE , taking a value of the order of few percent only for a step potential as high as $0.7\hbar\omega_c$ (note that, due to the non-zero reflection probability, $|t_{21}|^2$ slightly differs from $|t_{12}|^2$).

We mention that it is possible to calculate analytically the channel mixing scattering amplitudes in the limit of small step height $\Delta E \ll \hbar\omega_c$. Namely, we assume a potential of the form $U(y) = -\Delta E \Theta(y) e^{-y/\mathcal{L}}$ and take the limit $\mathcal{L} \rightarrow \infty$. It is possible to show that, up to a phase factor, the channel mixing amplitude t_{12} can be approximated to the first order in ΔE (Born approximation²³) as:

$$t_{12} = \frac{1}{\sqrt{\mathcal{N}_{12}}} \frac{\Delta E}{k_1^I - k_2^{II}} \int dx \psi_{k_1}^I(x) \psi_{k_2}^{*II}(x), \quad (11)$$

where

$$\mathcal{N}_{12} = \left| \int_0^L dx |\psi_{k_1}^I(x)|^2 (\beta x + k_1^I) \times \int_0^L dx' |\psi_{k_2}^{II}(x')|^2 (\beta x' + k_2^{II}) \right| \quad (12)$$

is the normalization factor that ensures the unitarity of the scattering matrix. We checked that the curve reported in Fig. 2 is fitted by the formula (11) close to the origin.

As a check we also consider the case of a single edge channel ($P_I = P_{II} = 1$). Here we have verified that the reflection probability $|r_{11}|^2$ is negligible, within the numerical accuracy, as long as L is greater than $6.5 l_B$. Current conservation therefore implies that one can write $t_{11} = e^{-i\phi}$.

The inset of Fig. 2 shows the phase ϕ in radians as a function of the potential step height ΔE in units of

$\hbar\omega_c$. The energy of the impinging electrons E_{eff}^I is set to $0.8\hbar\omega_c$ (*i.e.* $0.3\hbar\omega_c$ above the first LL). The phase shift ϕ increases monotonically nearly reaching the value $\pi/8$ for the highest step considered.

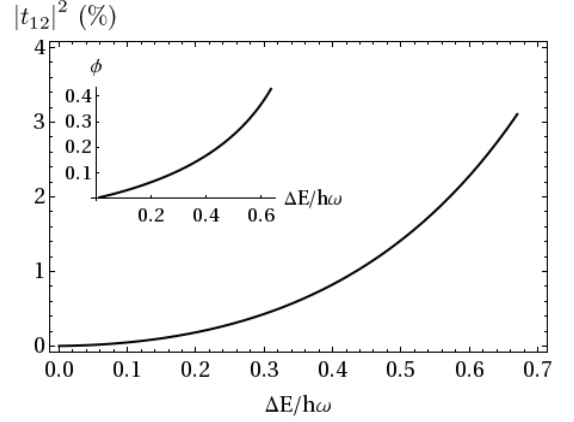


Figure 2: Channel mixing probability $|t_{12}|^2$ percentage, for the case $P_I = P_{II} = 2$, as a function of the height of the potential step ΔE . In the inset: scattering phase shift as a function of the potential step height for a single edge channel.

B. Series of potential steps

A possible strategy to achieve a channel mixing of the order of 50% is to place several potential steps in series. This is in principle possible by using nanopatterning techniques to realize a sequence of top gates. Assuming a typical magnetic lengths of about 10 nm, a few tens potential steps could be obtained over a length of some microns.

A simple evaluation of the channel-mixing transmission probability can be done by assuming that, after the sharp step, the potential smoothly goes to zero (see Fig. 3a). In doing so, after the mixing occurring at a potential step, the electrons in the two channels freely propagate along the potential tail to the next potential step accumulating a relative phase. Once suppressed all reflections due to the large separations between steps, the total transmission matrix $t(N)$ of a series of N steps is (up to a global phase) the product of the transmission matrices of the individual steps (of height ΔE_i) plus tails, which include the phase ϕ_i accumulated while propagating past the step i :

$$t(N) = \prod_{i=1}^N \begin{pmatrix} t_{11}(\Delta E_i) e^{i\phi_i} & t_{12}(\Delta E_i) e^{-i\phi_i} \\ t_{21}(\Delta E_i) e^{i\phi_i} & t_{22}(\Delta E_i) e^{-i\phi_i} \end{pmatrix}.$$

The phase ϕ_i depends both on the details of the adiabatic tail of the step and on the distance x_i between the steps. It turns out that even a few steps can increase dramatically the channel mixing probability $|t_{12}(N)|^2$ and that the latter very much depends on the set of phases

$\{\phi_i\}_{i=1,N}$. For example, 50% mixing can be achieved with four potential steps of height $\Delta E \simeq 0.72\hbar\omega_c$, or with 10 potential steps of height $\Delta E \simeq 0.4\hbar\omega_c$. The control of the phases ϕ_i , in order to tune the channel mixing, can be obtained by placing lateral finger gates in the region of the tail of the potentials. The role of these additional gates will be to modify the lateral confinement potential in such a way to alter the distance x_i traveled by the electrons propagating between two steps. Indeed, due to the large difference $(k_1^i - k_2^i)$, even a small variation of x_i (of the order of 1/10 of the magnetic length) results in a very significant variation of phase difference between the modes $\phi_i = (k_1^i - k_2^i)x_i \simeq 1$. In Fig. 3c the maximum (over ϕ_i) channel mixing probability $|t_{12}(N)|^2$ (obtained numerically) is plotted as a function of the number of potential steps for three different values of step height, namely $0.2\hbar\omega_c$, $0.4\hbar\omega_c$ and $0.72\hbar\omega_c$.

It is interesting to consider the situation where the phase differences ϕ_i are not controlled and take random values. In this case for every N one can average the channel mixing probability over a given number of configurations of the set $\{\phi_i\}_{i=1,N}$, with $\phi_i \in [0, 2\pi]$. In Fig. 3b we plot $|t_{12}(N)|^2$ averaged over 2000 configurations for different values of step height (the same as for Fig. 3c). We notice that equilibration (50% mixing) is reached for a large enough N .

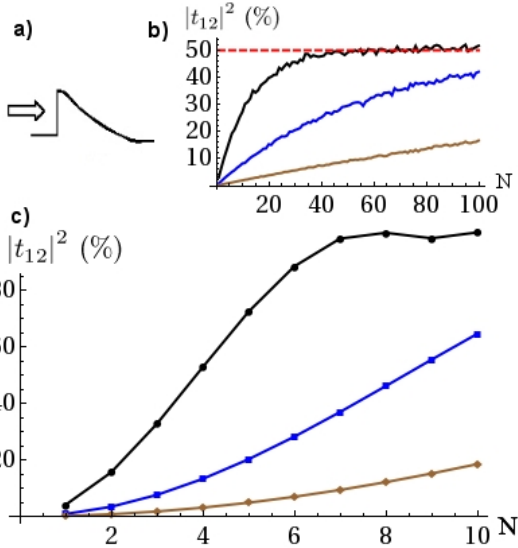


Figure 3: a) Single potential step followed by an adiabatic tail. b) Averaged channel mixing probability $|t_{12}|^2$ as a function of N for different potential heights (blue: $0.72\hbar\omega_c$, purple: $0.4\hbar\omega_c$, brown: $0.2\hbar\omega_c$) assuming random phases ϕ_i accumulated between the steps. Numerical error on unitarity of the S-matrix might induce variations of the order of 1%. The curves represent the average over 2000 random configurations. c) Channel mixing probability $|t_{12}|^2$ as a function of N for different potential heights (same color code as for panel b) assuming that each individual phase-adjusting gate is tuned to maximize the mixing.

C. Two regions with different filling factor

A second strategy for obtaining a significant channel mixing would consist in fixing $P_I = 1$ and setting ΔE large enough so that in region II two edge channels are open ($P_{II} = 2$). In this case the incoming electrons will be split between the two edge channels available in region II, according to the values of the transmission amplitudes t_{21} and t_{11} . Fig. 4 shows the probability $|t_{21}|^2$ for differ-

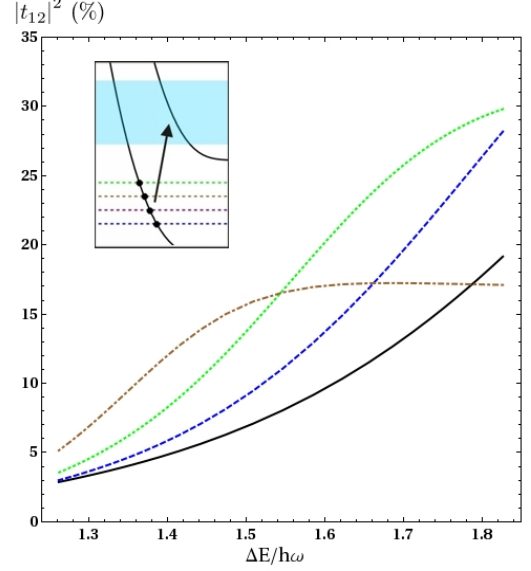


Figure 4: Channel mixing probability $|t_{12}|^2$ in the case where $P_I = 1$ and $P_{II} = 2$ for four different values of energy of the incoming electrons (pictured as dashed lines in the inset) as a function of the potential step height ΔE , which spans the energies indicated on the shaded area on the inset

ent values of incident energy E_{eff}^I and as a function of the energy step ΔE . For all the curves channel mixing exceeds 15 %, reaching about 30 % for $E_{eff}^I = 1.6\hbar\omega_c$ and $E_{eff}^I = 1.7\hbar\omega_c$.

We emphasize that this setup might be used to create the initial coherent superposition of wave-packet on the two edge channels which are needed for the interferometer of Ref. 10.

IV. ELECTRON PROBABILITY DENSITY

In this section we address the electron probability density $|\Psi(x,y)|^2$ in the case of two edge channels in region II ($P_{II} = 2$). In Fig. 5 the density $|\Psi(x,y)|^2$ is plotted in the case of a sharp step potential with $P_I = 2$ where electrons are injected from region I in channel 1 (a) and channel 2 (b). Vertical lines represent the position of the potential step ($y = 0$), so that region I is on the left hand side and region II is on the right hand side. Bright areas in region I correspond to the high probability den-

sity of incoming electrons exhibiting, in the transverse x -direction, one lobe, for injection from channel 1, and two lobes, for injection from channel 2. In region II the probability density relative only to the transmitted electronic wave functions with channel mixing is plotted, *i. e.* the contribution to the wave functions due to the amplitudes t_{11} (for panel (a)) and t_{22} (for panel (b)) has been subtracted for clarity.

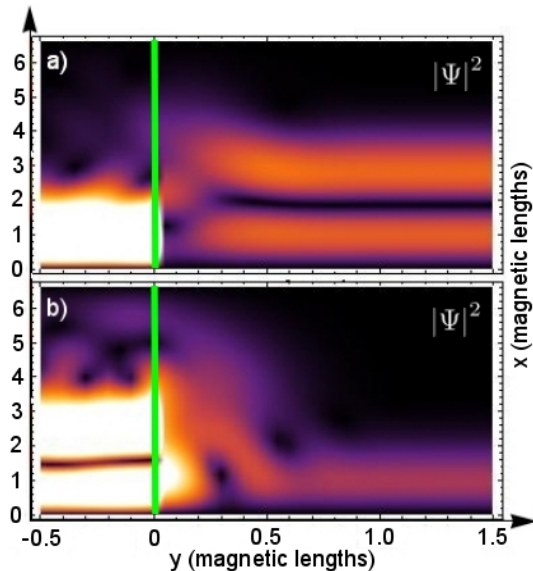


Figure 5: Charge probability density color plot of the edge states in the case where $P_I = 2$ and $P_{II} = 2$ with a sharp step potential. Vertical lines represent the position of the step potential. Electrons are injected from region I in channel 1 (a) and channel 2 (b). For the sake of clarity, only the contribution to the wave-function relative to t_{12} , for panel (a), and relative to t_{21} , for panel (b), are retained.

Up to now we have considered the ideal situation in which the step potential is sharp. Now we address the effect of the smoothening of the step and describe the cross-over to the adiabatic regime occurring when the potential varies over a length which is larger than the magnetic length. We make use of a tight-binding model where the wave-function is computed by means of the recursive Green's functions technique, applied successfully in other contexts²². Numerical simulations are performed by replacing the sharp step with a potential of the form $U(y) = -\Delta E/(e^{y/d} + 1)$, where d is the characteristic length (width) of the potential. In Fig. 6 contour plots of the probability density are shown when electrons are injected from the left in channel 1 for three different values of d , namely $d = 0.5l_B$ (a), $d = 1.3l_B$ (b) and $d = 3.5l_B$ (c). Vertical lines represent the center position of the smooth step potential. Figure 6(a) shows that, for $d = 0.5l_B$, there are beatings on the right hand side of the barrier which correspond to the coherent superposition of electronic waves over the two edge channels (the period of the oscillations corresponds to 2π divided by the difference of the wave-vectors of the two outgoing modes,

as expected). Such beatings are progressively suppressed as the barrier becomes smoother, eventually disappearing for $d = 3.5l_B$ (see Fig. 6c), when the edge channel injected from region I is totally transmitted to region II without mixing. It is worthwhile noting that the plot relative to $d = 0.5l_B$ is indistinguishable from the plot relative to a sharp edge. All simulations that we have performed confirm the picture of a crossover from the channel mixing situation to the adiabatic regime, reached when the potential step varies over a scale of a few magnetic lengths.

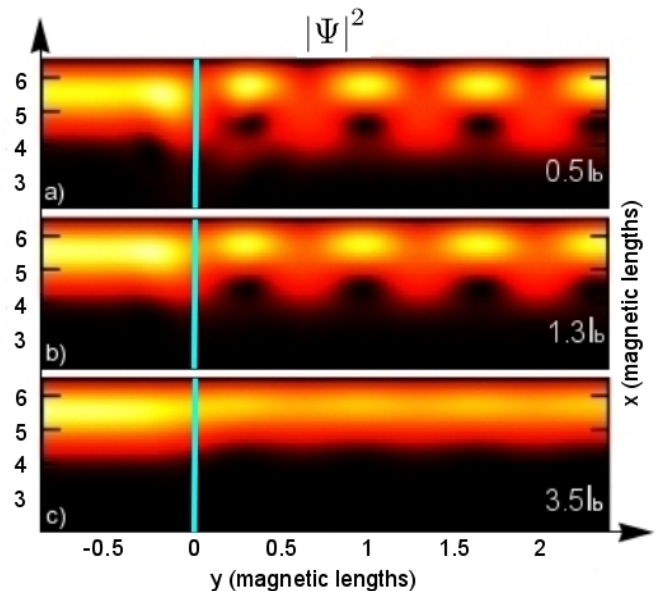


Figure 6: Charge probability density color plot of edge states in the case where $P_I = 1$ and $P_{II} = 2$ with a smooth step potential characterized by a width d indicated in figure. Vertical lines correspond to the center position of the step potential. Panel (a), (b) and (c) are relative to, respectively, $d=0.5$, 1.3 and 3.5 magnetic lengths. For $d = 0.5l_B$ the plot is indistinguishable from the one obtained with a sharp step.

V. CONCLUSIONS

In this paper we have investigated the edge channel mixing due to steps potentials in a 2DEG in the integer quantum Hall regime. In the case of a single sharp step we have found that, in the presence of two edge channels on each side of the step, the channel mixing probability cannot be larger than a few percent. Channel mixing, though, can be substantially enhanced by putting in series a small number of steps. More precisely, 50% mixing can be already be reached with 4 steps of large height, provided that one can control the phase accumulated by the electrons propagating between two consecutive steps. A quite large mixing can also be attained if the height of the steps is large enough to allow a single channel only on

its right hand side. Finally, we have addressed the effect of the step potential on the electron density probability even in the case where the step is smooth.

This work was by the Italian MIUR under the FIRB

IDEAS project RBID08B3FM, by the "Universita Italo Francese/Université Franco Italienne" (UIF/UFI) under the Program VINCI 2008 (chapter II), and by the ECOS-Sud program of French Government.

-
- ¹ M. Büttiker, Y. Imry, R. Landauer, and S. Pinhas, Phys. Rev. B **31**, 6207 (1985); M. Büttiker, *ibid.* **38**, 9375 (1988).
 - ² C. W. J. Beenakker and H. van Houten, Solid State Physics **44**, 1 (1991).
 - ³ P. Roulleau, F. Portier, D.C. Glatthli, P. Roche, A. Cavanna, G. Faini, U. Gennser, and D. Mailly, Phys. Rev. Lett. **100**, 126802 (2008).
 - ⁴ Y. Ji, et al., Nature **422**, 415 (2003).
 - ⁵ I. Neder, et al., Phys. Rev. Lett. **96**, 016804 (2006).
 - ⁶ L. V. Litvin, et al., Phys. Rev. B **75**, 033315 (2007).
 - ⁷ P. Roulleau, F. Portier, D. C. Glatthli, P. Roche, A. Cavanna, G. Faini, U. Gennser, and D. Mailly, Phys. Rev. B **76**, 161309(R) (2007).
 - ⁸ I. Neder et al., Nature Physics **3**, 534 (2007).
 - ⁹ I. Neder, et al., Nature **448**, 333 (2007).
 - ¹⁰ V. Giovannetti, F. Taddei, D. Frustaglia, and R. Fazio, Phys. Rev. B **77**, 155320 (2008).
 - ¹¹ L. I. Glazman and M. Jonson, Phys. Rev. B **41**, 10686 (1990).
 - ¹² Y. Ji, Y. Chung, D. Sprinzak, M. Heiblum, D. Mahalu, and H. Shtrikman, Nature (London) **422**, 415 (2003).
 - ¹³ I. Neder, N. Ofek, Y. Chung, M. Heiblum, D. Mahalu, and V. Umansky, Nature **448**, 333 .
 - ¹⁴ C. Altimiras, H. le Sueur, U. Gennser, A. Cavanna, D. Mailly, and F. Pierre, Nature Physics **6**, 34 (2009).
 - ¹⁵ D. Diaconescu, A. Goldschmidt, D. Reuter, and A. D. Wieck, Phys. Stat. Sol. (b) **245**, 276 (2008); R. Haug, A. D. Wieck, K. von Klitzing, and K. Ploog, Physica B **184**, 192 (1993).
 - ¹⁶ A. A. Shashkin, V. T. Dolgoplov, E. V. Deviatov, B. Irmer, A. G. C. Haubrich, J. P. Kotthaus, M. Bicher, and W. Wegscheider, JETP Lett. **69**, 603 (1999).
 - ¹⁷ M. Huber, M. Grayson, M. Rother, W. Biberacher, W. Wegscheider, and G. Abstreiter, Phys. Rev. Lett. **94**, 016805 (2005).
 - ¹⁸ N. Paradiso, S. Heun, S. Roddaro, L.N. Pfeiffer, K.W. West, L. Sorba, G. Biasol, F. Beltram, Physica E **42**, 1038 (2010).
 - ¹⁹ C. Tejedor and J. J. Palacios, Physica Scripta, **T35**, 121 (1991); J. J. Palacios and C. Tejedor, Phys. Rev. B **45**, 9059 (1992); J. J. Palacios and C. Tejedor, Phys. Rev. B **48**, 5386 (1993).
 - ²⁰ O. Olendski and L. Mikhailovska, Phys. Rev. B **72**, 235314 (2005).
 - ²¹ J. C. Barbosa and P. N. Butcher, Superlatt. Microstruct. **22**, 325 (1997).
 - ²² G. Usaj and C.A. Balseiro, Phys. Rev. B **70**, 041301(R) (2004).
 - ²³ M. Di Ventra, *Electrical Transport in Nanoscale Systems*, (Cambridge University Press, 2008).